Experimental Model Validation for a Flexible Robot With a Prismatic Joint

ARTICLE *in* JOURNAL OF MECHANICAL DESIGN · SEPTEMBER 1990

Impact Factor: 1.25 · DOI: 10.1115/1.2912610

3 AUTHORS, INCLUDING:

A. Galip Ulsoy
University of Michigan
287 PUBLICATIONS **6,047** CITATIONS
SEE PROFILE

Richard A. Scott
University of Michigan
89 PUBLICATIONS **1,823** CITATIONS
SEE PROFILE

Dynamic Modeling and Simulation of Flexible Robots With Prismatic Joints

Ye-Chen Pan*
Graduate Student.

R. A. Scott
Professor.
Mem. ASME

A. Galip Ulsoy
Associate Professor.
Mem. ASME

Department of Mechanical Engineering
and Applied Mechanics,
University of Michigan,
Ann Arbor, MI 48109-2125

A dynamic model for flexible manipulators with prismatic joints is presented in Part I of this study. Floating frames following a nominal rigid body motion are introduced to describe the kinematics of the flexible links. A Lagrangian approach is used in deriving the equations of motion. The work done by the rigid body axial force through the axial shortening of the link due to transverse deformations is included in the Lagrangian function. Kinematic constraint equations are used to describe the compatibility conditions associated with revolute joints and prismatic joints, and incorporated into the equations of motion by Lagrange multipliers. The small displacements due to the flexibility of the links are then discretized by a displacement based finite element method. Equations of motion are derived for the cases of prescribed rigid body motion as well as prescribed joint torques/forces through application of Lagrange's equations. The equations of motion and the constraint equations result in a set of differential algebraic equations. A numerical procedure combining a constraint stabilization method and a Newmark direct integration scheme is then applied to obtain the system response. An example, previously treated in the literature, is presented to validate the modeling and solution methods used in this study.

1 Introduction

In the past, manipulators were built to be rather massive, had high energy consumption and operated at low speed. Hence, the dynamic analysis of robotic arms was based upon rigid body assumptions [1, 2]. Owing to the demand to improve productivity and quality in industry, a considerable amount of interest has been focused on developing lightweight manipulators to reduce the driving torque requirement at high speed operation. However, the flexibility effect of the lightweight manipulators can cause problems such as degradation in accuracy, instability in the controller and material failure. In order to predict the dynamic response and provide better control action, a dynamic model which accounts for the flexibility of the links is needed.

Recently, a significant amount of effort has been reported on studies on the dynamics of robot arms taking into account the structural deformation. In these studies, small elastic deformations of the link are assumed, and either the finite element method or the assumed mode shapes method is used to describe the deformations of each individual link. The limitation of these studies is that they are applicable only to manipulators with revolute joints. Some studies have been done on flexible manipulators with prismatic joints, but they are limited to special, restricted cases. Another limitation in these studies is that only linear elastic deformations of the link are assumed; the nonlinear behavior due to axial shortening of the link resulting from the deformations is not taken into account.

The objective of this study is to develop a general dynamic model, taking into account the axial shortening effect of the link, for design and control of flexible manipulators with prismatic joints.

2 Previous Work

The research on the dynamic modeling of flexible manipulators originates from the study of flexible mechanisms and flexible spacecraft. In the 1970's, researchers in the field of spacecraft dynamics started studying the dynamic behavior of systems with elastic appendages [3, 4]. In these studies, elastic appendages were connected to a rigid body spinning at a prescribed rate.

In an earlier study of flexible manipulators [5], the masses of the elastic links were assumed to be negligible compared to the mass of the payload. This is true for manipulators, which are lightweight and operate at low speeds. However, this assumption cannot be applied to industrial manipulators, especially for higher operating speeds.

In recent years, a great deal of work has been devoted to the studies of planar flexible mechanisms, such as four-bar linkages and slider-rocker mechanisms [6–8], and spatial flexible mechanisms [9–12]. In these studies, small deformation of the links was assumed, and the finite element method was used to model the flexibility of the links.

Dubowsky and Sunada [13] extended their previous work

*Currently Senior Engineer, AeroStructures, Inc., Arlington, VA.

Contributed by the Mechanisms Committee for publication in the JOURNAL OF MECHANICAL DESIGN. Manuscript received August 1988; revised February 1989.

on spatial mechanisms [9] to flexible industrial manipulators. In that study, elastic motion is assumed to be a perturbation of a known nominal motion obtained from rigid body analysis. The distributed flexibility and mass properties of the links are modeled by the finite element method. Since the nominal motion is obtained from an independent rigid body analysis, their approach only provides one way coupling between the flexible motion and the rigid body motion. This limits its application to systems with such small deformations that flexible motions have little effect on the rigid body motions. Geradin, Robert, and Bernardin [14], provide two way coupling between the flexible motion and the rigid body motion. The nominal motion together with the flexible motion are solved from the coupled equations of motion.

Book [15] applied an assumed mode shapes method to model the flexibility of the links and derived a recursive form of the equations of motion for flexible manipulators. The two way coupling between rigid body motion and flexible motion was retained. However, no study on the accuracy of this model was presented. Judd and Falkenburg [16] later illustrated Book's procedure by deriving the equations of motions for a two-link planar robot. However, the kinetic energy due to the flexible motion was neglected to simplify the derivation.

All the research studies on flexible manipulators mentioned so far have been focused on manipulators with only revolute joints. Manipulators with prismatic joints are also widely used in industry. However, research on this type of robot has not received the attention it deserves.

Chalhoub and Ulsoy [17] presented simulations for a spherical coordinate manipulator with two revolute joints, one prismatic joint and a flexible link. Clamped-free mode shapes were used to model the vibrations of the links. In their model, the mode shapes were assumed to be time independent, and effects resulting from change of the length due to the prismatic joint were treated quasistatically. In Wang and Wei's work [18], a robot with a prismatic joint and a long flexible arm is modeled by a moving slender cantilever beam. The elastic motion of the beam is discretized by assumed time-dependent mode shapes. The effects of the axial force on the transverse vibration were included in the model and illustrated by examples. However, in that study, the rigid body motions of the robot arm were limited to prescribed rectilinear motions. The coupling effects are not fully provided for, and the effects of the rotational motions are not included.

As the dynamic behavior of flexible manipulators with only revolute joints have been fully studied in previous research work, it is necessary to develop a general approach to obtain dynamic models for flexible robot arms with prismatic as well as revolute joints.

3 Formulation

The robotic manipulators in this study are assumed to consist of a sequence of links connected either by revolute joints or prismatic joints. The numbering of the links and joints is as follows: link 1, the first link, is connected to the ground (link 0) by joint 1 and accordingly link i is connected to link i-1 by joint i.

The elastic motion of the flexible manipulator is considered as a small perturbation about a nominal motion generated by a hypothetical robot. The mass and dimensions of the links of this hypothetical robot are the same as the flexible manipulator except that all the links of the hypothetical robot are assumed to be rigid. To measure the deformation of each link, a set of axes from which to measure the deformation of the link has to be specified. If an inertially fixed set of axes is chosen, the displacements relative to these axes may grow large since the links are undergoing large rotation and translation. Then the dynamic analysis using these displacements may require nonlinear expressions to describe the relation between the displacement and strain. In order to simplify the analysis, frames which, in some way, move with the links are used to measure the deformations of the links. If these frames, called floating frames, move with the links or "float" in a proper way, the displacement measured relative to these frames will be small. Hence, linear expressions relating the displacements and strains can be used [4]. It has been pointed out by Canavin and Likins [4] that the Tisserand frame is the most advantageous choice of the floating frames in the study of flexible spacecraft. However, due to the kinematic structures of robotic manipulators, researchers use locally attached frames to study the dynamics of flexible robots. Sunada, Dubowsky [13], and Geradin, Robert, and Bernardin [14] used locally attached frames following the nominal rigid body motions. Book [5] used locally attached frames following the actual motions of the manipulator. Geradin, Robert, and Bernardin [14] also pointed out that the frames following the nominal rigid body motions provide weaker coupling between the rigid body degrees of freedom and the elastic degrees of freedom, and lead to a better form of the equations of motion for finite element modeling than those following the actual motions. Hence, floating frames following the nominal motions are adopted in this study. These frames are attached to the links of the hypothetical rigid manipulator to describe the actual configuration of the flexible manipulator. Floating frame i is attached to the left end of link i of the hypothetical rigid robot in such a way that its X_i-axis is aligned with the link.

To illustrate this concept, consider a 2-link flexible robot with one revolute joint and one prismatic joint. Figure 1 shows the configurations of both the flexible manipulator and the hypothetical rigid body robot at time instant t. Link 1 and link 2 are the two links of the flexible manipulator while link 1′ and link 2′ are the links of the hypothetical rigid body manipulator. The variables θ and s are the joint angle and joint displacement of the revolute joint and the prismatic joint of the rigid manipulator, respectively. For the case of prescribed motion, the time histories of θ and s are assumed to be known beforehand through a rigid body analysis. The inertial frame X_0-Y_0-Z_0 is set up at the first joint. Two floating frames are attached to the manipulator. Frame 1, X_1-Y_1-Z_1,

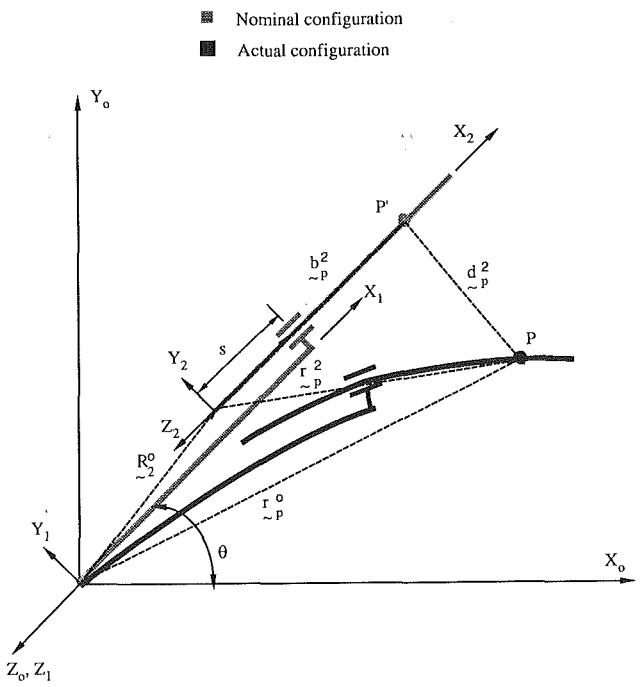

Fig. 1 Schematic of a two-link robot

is attached to the left end of link 1′ with the X_1-axis aligned with the link, and frame 2, X_2-Y_2-Z_2, is attached to link 2′ in a similar way. Floating frames 1 and 2 move with links 1′ and 2′, respectively. The small displacements due to the flexibility of the links are measured from these floating frames and the configuration of each link is first referred to its own local floating frame and then referred to the inertial frame X_0-Y_0-Z_0 by coordinate transformations through rotation matrices.

The position of a generic point P on link i with respect to the inertial frame, as illustrated in Fig. 1, can be written in vector form, as:

$$\mathbf{r}_p^0 = \mathbf{R}_i^0 + \mathbf{b}_p^i + \mathbf{d}_p^i \tag{1}$$

where $\mathbf{r}_p^0$ is the position vector of P w.r.t. the inertial frame, $\mathbf{R}_i^0$ is the position vector of the origin of frame i w.r.t. the inertial frame, $\mathbf{b}_p^i$ is the position vector of P in its undeformed state (i.e., P') w.r.t. the ith frame, and $\mathbf{d}_p^i$ is the position vector of the small displacement, resulting from the flexibility of the links, w.r.t. the ith floating frame. Note that the small displacement $\mathbf{d}_p^i$ is not only due to the deformation of link i but also due to the deformations of the links prior to link i. Equation (1) can also be expressed in matrix form through the use of a rotation matrix:

$$\{\mathbf{r}_p^0\} = \{\mathbf{R}_i^0\} + [A_0^i](\{\mathbf{b}_p^i\} + \{\mathbf{d}_p^i\}) \tag{2}$$

where $\{\mathbf{r}_p^0\} = \{x_p^0, y_p^0, z_p^0\}^T$ is the coordinate of P w.r.t. the inertial frame, $\{\mathbf{R}_i^0\} = \{X_i^0, Y_i^0, Z_i^0\}^T$ is the coordinate of the origin of the ith frame w.r.t. the inertial frame, $[A_0^i]$ is the rotation matrix between the inertial frame and the ith frame, $\{\mathbf{b}_p^i\} = \{\mathbf{b}_p^i, 0, 0\}^T$ gives the coordinates of P' w.r.t. the ith frame, and $\{\mathbf{d}_p^i\} = \{u_p^i, v_p^i, w_p^i\}^T$ contains the components of the small displacement of P w.r.t. the ith frame.

The velocity and acceleration of point P can be obtained by taking the first and second derivative with respect to time of (2):

$$\{\dot{\mathbf{r}}_p^0\} = \{\dot{\mathbf{R}}_i^0\} + [\dot{A}_0^i](\{\mathbf{b}_p^i\} + \{\mathbf{d}_p^i\}) + [A_0^i]\{\dot{\mathbf{d}}_p^i\} \tag{3}$$

Noting that $\{\dot{\mathbf{b}}_p^i\} \equiv 0$, the acceleration is given by,

$$\{\ddot{\mathbf{r}}_p^0\} = \{\ddot{\mathbf{R}}_i^0\} + [\ddot{A}_0^i](\{\mathbf{b}_p^i\} + \{\mathbf{d}_p^i\}) + 2[\dot{A}_0^i]\{\dot{\mathbf{d}}_p^i\} + [A_0^i]\{\ddot{\mathbf{d}}_p^i\} \tag{4}$$

Since P is a generic point, we can drop the subscript p in (2), (3) and (4) to obtain the expressions for the energy terms. The kinetic energy of link i is defined as

$$T_i = \frac{1}{2}\int_{m_i} \{\dot{\mathbf{r}}^0\}^T\{\dot{\mathbf{r}}^0\}\,dm_i \tag{5}$$

Substituting (3) into (5) and assuming constant mass density, we get

$$T_i = \frac{\rho_i}{2}\int_{v_i} [\{\dot{\mathbf{R}}_i^0\}^T + (\{\mathbf{b}^i\}^T + \{\mathbf{d}^i\}^T)[\dot{A}_0^i]^T + \{\dot{\mathbf{d}}^i\}^T[A_0^i]^T][\{\dot{\mathbf{R}}_i^0\} + [\dot{A}_0^i](\{\mathbf{b}^i\} + \{\mathbf{d}^i\}) + [A_0^i]\{\dot{\mathbf{d}}^i\}]dv \tag{6}$$

where ρ_i is the mass density of link i. The payload is modeled as a concentrated mass attached at the tip of the last link (link m). Hence, the kinetic energy of the payload is

$$T_t = \frac{1}{2} M_t\{\dot{\mathbf{r}}_t^0\}^T\{\dot{\mathbf{r}}_t^0\} \tag{7}$$

where M_t is the mass of the payload, and $\{\dot{\mathbf{r}}_t^0\}$ can be obtained from (3) with $i = m$.

The potential energy of a flexible manipulator consists of three terms: gravitational potential energy, strain energy based on small strain theory, and the work done by the axial forces arising from the axial shortening of the link. The gravitational potential energy (w.r.t. the X_0-Z_0 plane) of link i is defined by

$$V_i|_g = \rho_i\int_{v_i} \{\mathbf{g}\}^T\{\mathbf{r}^0\}\,dv$$

$$= \rho_i\int_{v_i} \{\mathbf{g}\}^T(\{\mathbf{R}_i^0\} + [A_0^i]\{\mathbf{b}^i\} + [A_0^i]\{\mathbf{d}^i\})\,dv \tag{8}$$

where $\{\mathbf{g}\}^T = \{\mathbf{g}_x, \mathbf{g}_y, \mathbf{g}_z\}^T$ contains the components of the acceleration due to gravity. The gravitational potential energy of the payload is

$$V_t|_g = M_t\{\mathbf{g}\}^T(\{\mathbf{R}_m^0\} + [A_0^m]\{\mathbf{b}_t^m\} + [A_0^m]\{\mathbf{d}_t^m\}) \tag{9}$$

Since small elastic deformations are assumed, and both shear deformations and rotary inertia are neglected, the strain energy of link i can be obtained from small strain theory [19]:

$$V_i|_\epsilon = \frac{1}{2}\int_0^{L_i} \left(E_i a_i\left(\frac{\partial u^i}{\partial x}\right)^2 + E_i I_y\left(\frac{\partial^2 v^i}{\partial x^2}\right)^2 + E_i I_z\left(\frac{\partial^2 w^i}{\partial x^2}\right)^2 + G_i J_i\left(\frac{\partial \phi_x^i}{\partial x}\right)^2\right)dx \tag{10}$$

where L_i is the length of link i, a_i is the cross sectional area of link i, E_i is the Young's modulus of link i, I_y, I_Z are the area moment of inertias of link i, G_iJ_i is the torsional rigidity of link i, u^i, v^i, w^i, are the components of the small displacement resulting from the flexibility of the links as described in (2), and ϕ_x^i is the angle of twist of link i.

The expression for the strain energy of the links in (10) was derived based on small strain theory. In that theory, the transverse deformation is considered independent of the force in the axial direction. However, at high speed operation, especially when axial rigid body motions are involved, the influence of the axial forces on the transverse deformations becomes significant. This effect can be taken into account by including higher order terms in the elastic strain energy in finite element methods. However, as noted by Nath and Ghosh [6], this procedure cannot allow for variations of the rigid body axial force along the link. The procedure adopted here is the one used in Meirovitch [20]. The effect of axial shortening is taken into account by computing the work done by the axial forces acting through the distance,

$$dL = ds - dx \tag{11}$$

where ds is the length of the differential element after deformation, and dx is the projection of the differential element in the axial direction. Now, referring to Fig. 2 one may write

$$ds = dx\sqrt{1 + \left(\frac{\partial w}{\partial x}\right)^2} \tag{12}$$

Assuming small $\frac{\partial w}{\partial x}$, a binomial expansion gives

$$ds \cong dx\left[1 + \frac{1}{2}\left(\frac{\partial w}{\partial x}\right)^2\right] \tag{13}$$

Substituting (13) into (11), we obtain

$$dL \cong \frac{1}{2}\left(\frac{\partial w}{\partial x}\right)^2 dx \tag{14}$$

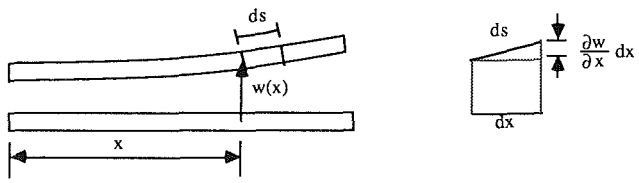

Fig. 2 Axial shortening of a beam under plane transverse deflection

In the nonplanar case, dL can be similarly approximated by

$$dL \cong \frac{1}{2}\left[\left(\frac{\partial v}{\partial x}\right)^2 + \left(\frac{\partial w}{\partial x}\right)^2\right]dx \tag{15}$$

The axial force F_i (due to inertial forces and gravity) does an amount of work $F_i dL$. Hence, the associated potential energy of link i is

$$V_i|_a = \int F_i(x)dL \cong \frac{1}{2}\int_0^{L_i} F_i(x)\left[\left(\frac{\partial v^i}{\partial x}\right)^2 + \left(\frac{\partial w^i}{\partial x}\right)^2\right]dx \tag{16}$$

Since the elastic motion is considered to be a small perturbation of the nominal rigid body motion, the inertial force due to the elastic motion can be neglected. The axial forces along link i can be obtained using (4) and neglecting the elastic motion:

$$F_i(x) = -\rho_i a_i \int_x^{L_i} \{\mathbf{e}_x\}^T[\mathrm{A}_0^i]^T(\{\ddot{\mathbf{R}}_i^0\} + [\ddot{A}_0^i]\{\mathbf{b}^i\} + \{\mathbf{g}\})d\xi - H_i \tag{17}$$

where $\{\mathbf{e}_x\} = \{1, 0, 0\}^T$, $\{\mathbf{b}^i\} = \{\xi, 0, 0\}^T$, and

$$H_i = \{\mathbf{e}_x\}^T[\mathrm{A}_0^i]^T \sum_{k=i+1}^{m} (\rho_k a_k \int_0^{L_k} (\{\ddot{\mathbf{R}}_k^0\} + [\ddot{A}_0^k]\{\mathbf{b}^k\} + \{\mathbf{g}\})d\xi) + M_t\{\mathbf{e}_x\}^T[A_0^m]^T(\{\ddot{\mathbf{R}}_m^0\} + [\ddot{A}_0^m]\{\mathbf{b}_t^m\} + \{\mathbf{g}\})$$

H_i accounts for the additional axial forces which come from the payload and the links after link i. For the last link, (17) yields

$$F_m(x) = -\rho_m a_m \int_x^{L_m} \{\mathbf{e}_x\}^T[A_0^m]^T(\{\ddot{\mathbf{R}}_m^0\} + [\ddot{A}_0^m]\{\mathbf{b}^m\} + \{\mathbf{g}\})d\xi - M_t\{\mathbf{e}_x\}^T[A_0^m]^T(\{\ddot{\mathbf{R}}_m^0\} + [\ddot{A}_0^m]\{\mathbf{b}_t^m\} + \{\mathbf{g}\}) \tag{18}$$

So far, the expressions for the kinetic energy and potential energy have been derived as if each link were independent of the others. The joints connecting the adjacent links were not taken into account. In the following discussion, the compatibility conditions arising from the revolute joints and prismatic joints between the links are described by the kinematic constraint equations. These constraint equations are then incorporated into Lagrange's equations through the use of Lagrange multipliers.

A revolute joint i connecting link i and link $i-1$ is shown in Fig. 3, where joint i' is the corresponding joint on the hypothetical rigid robot. The small displacement due to the flexibility of the links must be continuous at the joint, that is, the small displacement of joint i measured from frame $i-1$ must be the same as that measured from frame i. This yields:

$$\{\mathbf{d}_r^{i-1}\} = [A_{i-1}^i]\{\mathbf{d}_l^i\} \tag{19}$$

where $\{\mathbf{d}_r^{i-1}\} = \{u_r^{i-1}, v_r^{i-1}, w_r^{i-1}\}^T$ is the small displacement at the right end of link $i-1$ measured w.r.t. frame $i-1$, and $\{\mathbf{d}_l^i\} = \{u_l^i, v_l^i, w_l^i\}^T$ is the small displacement at the left end of link i measured w.r.t. frame i.

Another compatibility condition associated with the revolute joint is that the adjacent links share a common axis of rotation at the joint. The kinematic constraint equations corresponding to this condition yield [21]:

$$\phi_{yr}^{i-1} = \phi_{yl}^i\cos\theta_i + \phi_{xl}^i\sin\theta_i \tag{20}$$

$$\phi_{xr}^{i-1} = -\phi_{yl}^i\sin\theta_i + \phi_{xl}^i\cos\theta_i \tag{21}$$

where ϕ_{xl}^i is the angle of twist at the left end of link i measured w.r.t. frame i, ϕ_{xr}^{i-1} is the angle of twist at the right end of link $i-1$ measured w.r.t. frame $i-1$, $\phi_{yl}^i \equiv -\partial w_l^i/\partial x$, $\phi_{yr}^{i-1} \equiv -\partial w_r^{i-1}/\partial x$, and θ_i is the nominal joint angle of joint i.

Two common types of prismatic joints used in industrial robots are shown in Fig. 4 and Fig. 5. In Fig. 4, link i moves in and out of link $i-1$ which is rigid. For the prismatic joint in Fig. 5, link i and link $i-1$ can both be flexible. The compatibility conditions of the prismatic joint shown in Fig. 4 require that the elastic displacements, slopes at the left end of link i and angle of twist to be zero. Also the transverse displacements of point D' on the neutral axis of link i at the bilateral support is zero. The kinematic constraint equations describing these types of prismatic joints are:

$$\{\mathbf{d}_l^i\} = 0 \tag{22}$$

$$\frac{\partial v_l^i}{\partial x} = \frac{\partial w_l^i}{\partial x} = \phi_{xl}^i = 0 \tag{23}$$

and

$$v_{D'}^i = 0 \tag{24}$$

$$w_{D'}^i = 0 \tag{25}$$

Note that, point D' is changing with time since link i is moving relative to link $i-1$. For the prismatic joint shown in Fig. 5, the compatibility conditions require that the small displacements at the joint due to the flexibility to be the same for both links. Furthermore, the rotations about the Y_{i-1}-axis and the Z_{i-1}-axis are the same when measured from frame i and from frame $i-1$. The kinematic constraint equations are:

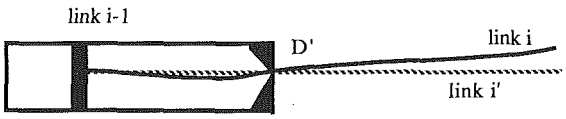

Fig. 4 Schematic of prismatic joint i

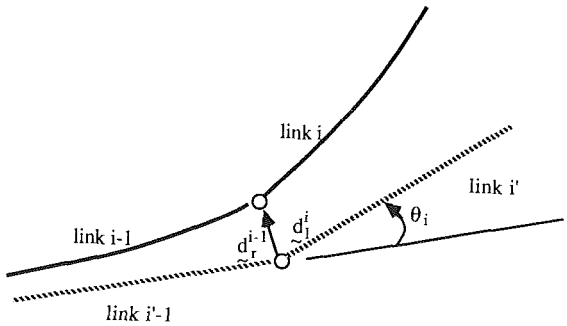

Fig. 3 Schematic of revolute joint i

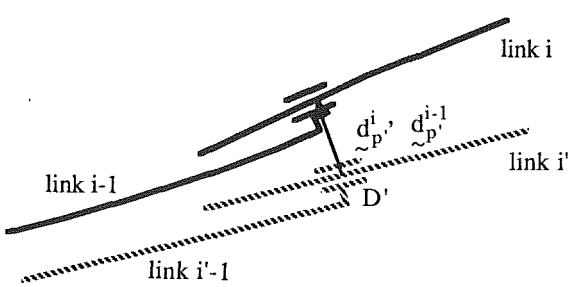

Fig. 5 Schematic of prismatic joint i

$$\{\mathbf{d}_{D'}^{i-1}\} = \{\mathbf{d}_{D'}^{i}\} \tag{26}$$

$$\left(\frac{\partial v_{D'}^{i-1}}{\partial x}\right) = \left(\frac{\partial v_{D'}^{i}}{\partial x}\right) \tag{27}$$

$$\left(\frac{\partial w_{D'}^{i-1}}{\partial x}\right) = \left(\frac{\partial w_{D'}^{i}}{\partial x}\right) \tag{28}$$

Again, the point D' is changing with time due to the translational motion of link i.

To derive equations of motion, the small displacements resulting from the flexibility of the links are spatially discretized using a finite element method and then Lagrange's equations are applied. In the present study, the links of the robot are treated as long slender beams. Hence, each flexible link is discretized into a number of simple beam elements. Considering an m-link robot, the ith link is divided into m_i simple beam elements. The small displacement of a point a distance ζ away from the left end of the jth beam element on link i can be expressed as [22]:

$$\{\mathbf{d}^i\} = [N(\zeta)]\{\mathbf{q}\}_{(i)}^{(j)} \tag{29}$$

where $\{\mathbf{d}^i\}$ is the small displacement resulting from the flexibility of the link i as described in (2), $\{\mathbf{q}\}_{(i)}^{(j)}$ is the nodal degrees of freedom of the jth beam element on link i, and $[N(\zeta)]$ is the standard shape function matrix of the beam element.

Applying the finite element discretization, and using (6), the kinetic energy of link i can be written as,

$$\begin{aligned}
T_i = \frac{\rho_i}{2}\sum_{j=1}^{m_i}\Bigg(\int_{v_{ij}} & \{\dot{\mathbf{R}}_i^0\}^T\{\dot{\mathbf{R}}_i^0\} + 2\{\dot{\mathbf{R}}_i^0\}^T[\dot{A}_0^i]\{\mathbf{b}^i\}^{(j)} \\
& + 2\{\dot{\mathbf{R}}_i^0\}^T[\dot{A}_0^i][N]\{\mathbf{q}\}_{(i)}^{(j)} \\
& + 2\{\dot{\mathbf{R}}_i^0\}^T[A_0^i][N]\{\dot{\mathbf{q}}\}_{(i)}^{(j)} + \{\mathbf{q}\}_{(i)}^{(j)T}[N]^T[\dot{A}_0^i]^T[\dot{A}_0^i][N]\{\mathbf{q}\}_{(i)}^{(j)} \\
& + \{\mathbf{b}^i\}^{(j)T}[\dot{A}_0^i]^T[\dot{A}_0^i]\{\mathbf{b}^i\}^{(j)} + 2\{\mathbf{q}\}_{(i)}^{(j)T}[N]^T[\dot{A}_0^i]^T[\dot{A}_0^i]\{\mathbf{b}^i\}^{(j)} \\
& + 2\{\mathbf{q}\}_{(i)}^{(j)T}[N]^T[\dot{A}_0^i]^T[A_0^i][N]\{\dot{\mathbf{q}}\}_{(i)}^{(j)} \\
& + 2\{\mathbf{b}^i\}^{(j)T}[\dot{A}_0^i]^T[A_0^i][N]\{\dot{\mathbf{q}}\}_{(i)}^{(j)} \\
& + \{\dot{\mathbf{q}}\}_{(i)}^{(j)T}[N]^T[N]\{\dot{\mathbf{q}}\}_{(i)}^{(j)T}dv\Bigg)
\end{aligned} \tag{30}$$

where v_j is the volume of element j, and

$$\{\mathbf{b}^i\}^{(j)} = \{\zeta, 0, 0\}^T \qquad \text{for } j=1.$$

$$= \left[\sum_{k=1}^{j-1} 1_{ik} + \zeta, 0, 0\right]^T \qquad \text{for } j>1.$$

The potential energy of link i is

$$V_i = V_i|_g + V_i|_\epsilon + V_i|_a \tag{31}$$

The contributions to the potential energy of link i from $V_i|_g$ and $V_i|_\epsilon$ become, using (8) and (10),

$$V_i|_g = \rho_i\sum_{j=1}^{m_i}\left(\int_{v_{ij}}\{\mathbf{g}\}^T(\{\mathbf{R}_i^0\} + [A_0^i\{\mathbf{b}^i\}^{(j)} + [A_0^i]\{\mathbf{q}\}_{(i)}^{(j)})dv\right) \tag{32}$$

$$V_i|_\epsilon = \frac{1}{2}\sum_{j=1}^{m_i}\{\mathbf{q}\}_{(i)}^{(j)T}[K_{ij}]\{\mathbf{q}\}_{(i)}^{(j)} \tag{33}$$

where $[K_{ij}]$ is the element stiffness matrix. In evaluating the work done by the axial force, the length of the element is regarded as the length of the neutral axis. Since the transverse displacement of the neutral axis is independent of the angle of twist, the influence of the angle of twist can be neglected in discretizing the expression for $V_i|_a$. A separate discretization is performed for (16), namely,

$$V_i|_a = \frac{1}{2}\sum_{j=1}^{m_i}\int_0^{l_{ij}} F_j(\zeta)\{\mathbf{q}\}_{(i)}^{(j)T}[\underline{N}']^T[\underline{N}']\{\mathbf{q}\}_{(i)}^{(j)}d\zeta \tag{34}$$

where $[\underline{N}(\zeta)]$ is a modified shape function matrix [21], $[\underline{N}'] = \frac{d}{d\zeta}[\underline{N}]$, and

$$F_j(\zeta) = -\rho_i a_i\int_x^{L_i}\{\mathbf{e}_x\}^T[A_0^i]^T(\{\ddot{\mathbf{R}}_i\} + [\ddot{A}_0^i]\{\mathbf{b}^i\})d\xi - H_i$$

$$x=\zeta \qquad \text{for } j=1.$$

$$= \sum_{k=1}^{j-1} 1_{ik} + \zeta \qquad \text{for } j>1.$$

In the case of prescribed torques/forces, the nominal joint motions need to be solved together with the flexible motions. Hence, the generalized coordinates of the system in this case must contain both nodal degrees of freedom and nominal joint angles/displacements, i.e.,

$$\{\mathbf{q}\} = \{\{\mathbf{q}\}_{(1)}^T, \{\mathbf{q}\}_{(2)}^T, \ldots, \{\mathbf{q}\}_{(m)}^T, \{\mathbf{q}\}_{(R)}^T\}^T \tag{35}$$

where $\{\mathbf{q}\}_{(R)}$ is a $m \times 1$ vector of the nominal joint angles and joint displacements, and $\{\mathbf{q}\}_{(i)}$ is a column vector containing nodal degrees of freedom of link i. In the case of prescribed motions, the nominal joint angles and joint displacements are given functions of time. Hence, the generalized coordinates of the system become

$$\{\mathbf{q}\} = \{\{\mathbf{q}\}_{(1)}^T, \{\mathbf{q}\}_{(2)}^T, \ldots, \{\mathbf{q}\}_{(m)}^T\}^T \tag{36}$$

With the generalized coordinates in (35) or (36), the kinematic constraint equations associated with the joints can be written in the general form:

$$\Phi_j(\{\mathbf{q}\}, t) = 0, \qquad j = 1, \ldots, n_c \tag{37}$$

where n_c is the number of the constraint equations. Equation (37) may be written also in a column vector form,

$$\{\Phi(\{\mathbf{q}\}, t)\} = 0 \tag{38}$$

The system kinetic energy and potential energy can be obtained by summing up the energy of each link:

$$T = \sum_{i=1}^{m} T_i + T_t \tag{39}$$

$$V = \sum_{i=1}^{m} V_i + V_t \tag{40}$$

The Lagrangian function $\mathbf{L}$ of the system can be written as

$$\mathbf{L} = T - V = \sum_{i=1}^{m} T_i + T_t - \sum_{i=1}^{m} V_i - V_t \tag{41}$$

Equations of motion are derived for the case of prescribed motion as well as the case of prescribed torques/forces. The assumption underlying the prescribed motion case is that the flexible motions have a negligible effect on the rigid body motions. Under these circumstances, the equations of rigid body dynamics can be used to obtain the motions from the applied forces and torques. Then the generalized coordinates are given by (36) and Lagrange's equations become, using Lagrange multipliers to deal with the constraint equations,

$$\frac{d}{dt}(\partial \mathbf{L}/\partial \dot{q}_j) - \frac{\partial \mathbf{L}}{\partial q_j} + \sum_{i=1}^{nc} \lambda_i \frac{\partial \Phi_i}{\partial q_j} = 0 \quad j = 1, \ldots, n_e \tag{42}$$

where q_j is the generalized coordinate (also the nodal displacement), Φ_i $(\{\mathbf{q}\}, t) = 0$, $(i = 1, \ldots, n_c)$ are the kinematic constraint equations, λ_i is the Lagrange multiplier associated with the constraint equation, and n_e is the number of generalized coordinates.

In the case of prescribed torques/forces, the nominal rigid body motions need to be solved together with the nodal displacements from the equations of motion. Complete coupling between the rigid body and elastic motions is thus retained. The equations of motion are obtained by applying Lagrange's equations:

$$\frac{d}{dt}(\partial \mathbf{L}/\partial \dot{q}_j) - \frac{\partial \mathbf{L}}{\partial q_j} + \sum_{i=1}^{nc} \lambda_i \frac{\partial \Phi_i}{\partial q_j} = \{\mathbf{Q}\} \quad j = 1, \ldots, n \tag{43}$$

where the q_j are the generalized coordinates as described in (35), $\{\mathbf{Q}\}$ is a column vector containing the generalized forces/torques resulting from actuator actions, $n = n_e + n_r$ is the number of generalized coordinates, and n_r is the number of generalized coordinates associated with the nominal rigid body motion.

4 Numerical Procedure

The general form of the equations of motion and the kinematic constraint equations derived in the previous section can be expressed as n second order differential equations with m holonomic constraint equations:

$$[M]\{\ddot{\mathbf{q}}\} + \Phi_q]^T\{\lambda\} = \{\mathbf{f}\} \tag{44}$$

$$\{\Phi(\{\mathbf{q}\}, t\} = 0 \tag{45}$$

where $[M]$ is an $n \times n$ generalized mass matrix, $\{\Phi\}$ is an $m \times 1$ vector containing m independent constraint equations, $\{\lambda\}$ is an $m \times 1$ vector containing the Lagrange multipliers associated with the m constraint equations, $\{\mathbf{f}\}$ is an $n \times 1$ vector of generalized forces, $\{\mathbf{q}\}$ is an $n \times 1$ vector of generalized coordinates, and $[\Phi_q]$ is an $m \times n$ Jacobian matrix of the kinematic constraint equations with elements $[\Phi_q]_{ij} = \partial \Phi_i / \partial q_j$.

Equations (44), (45) constitute a system of differential algebraic equations (DAE) of index 3 [24]. The index characterizes the structure of the DAE system. Systems with higher indices are more difficult to solve numerically than those with lower indices [25, 26]. Due to the numerical difficulty in solving index 3 systems, researchers do not tackle the original unmodified system of (44) and (45). Instead the index of the system is lowered to 1 by differentiating the constraint equation (45) twice, and then employing some special methods to solve the resulting modified index 1 system [11, 27-29].

Here, the index of the system is first lowered to 1 and then a numerical procedure combining a constraint stabilization method proposed by Baumgarte [27] and a Newmark direct integration method are employed. Computer runs showed the current method to be more efficient than existing codes based on Gear's algorithm. The constraint stabilization method feeds back the violations of the position and velocity constraints to "damp out" the violations at the current step, and the Newmark method is used to ensure the stability of the integration.

Taking the first and second time derivatives of (45), one obtains velocity and acceleration constraint equations:

$$[\Phi_q]\{\dot{\mathbf{q}}\} = -\{\Phi_t\} \tag{46}$$

$$[\Phi_q]\{\ddot{\mathbf{q}}\} = \{\mathbf{h}\} \tag{47}$$

where

$$[\Phi_t] = \partial\{\Phi\}/\partial t$$

$$\{\mathbf{h}\} = -[\Psi_q]\{\dot{\mathbf{q}}\} - 2[\Phi_{qt}]\{\dot{\mathbf{q}}\} - \{\Phi_{tt}\}$$

$$[\Psi_q]_{ij} = \partial([\Phi_q]\{\dot{\mathbf{q}}\})_i/\partial q_j$$

The initial conditions $\{\mathbf{q}(0)\} = \{\mathbf{q}\}_0$, $\{\dot{\mathbf{q}}(0)\} = \{\dot{\mathbf{q}}\}_0$ must satisfy (45) and (46), and cannot be arbitrarily assigned. With (44) and (47), a system of differential algebraic equations, in $\{\mathbf{q}\}$ and $\{\lambda\}$, of index 1 is constructed.

$$\begin{bmatrix} [M] & [\Phi_q]^T \\ [\Phi_q] & [0] \end{bmatrix} \begin{Bmatrix} \{\ddot{\mathbf{q}}\} \\ \{\lambda\} \end{Bmatrix} = \begin{Bmatrix} \{\mathbf{f}\} \\ \{\mathbf{h}\} \end{Bmatrix} \tag{48}$$

The constraint stabilization method allows constraints to be violated slightly before corrective action takes place. An outline of the procedure is as follows: $\{\dot{\mathbf{q}}\}$ and $\{\mathbf{q}\}$ are used to generate $\{\dot{\Phi}\}$ and $\{\Phi\}$, which are not identically zero because of numerical errors. These terms are then fed back to the acceleration constraint equation (47) to generate the modified form:

$$[\Phi_q]\{\ddot{\mathbf{q}}\} = \{\mathbf{h}\} - 2\gamma\{\dot{\Phi}\} - \beta^2\{\Phi\} \tag{49}$$

where γ and β are positive parameters to be chosen to improve accuracy. Nikravesh [28] suggested taking $\gamma = \beta$, with γ in the range of 5 to 50. In this study, a value of $\gamma = \beta = 5$ was found to be satisfactory and used to obtain all the numerical results.

In the Newmark direct integration method, the acceleration and velocity at the $i+1$th time step can be expressed as [22],

$$\{\ddot{\mathbf{q}}\}^{i+1} = \frac{1}{\alpha(\Delta t)^2}(\{\mathbf{q}\}^{i+1} - \{\mathbf{q}\}_i) - \frac{1}{\alpha \Delta t}\{\dot{\mathbf{q}}\}_i - \left(\frac{1}{2\alpha} - 1\right)\{\ddot{\mathbf{q}}\}^i \tag{50}$$

$$\{\dot{\mathbf{q}}\}^{i+1} = \left(1 - \frac{\delta}{\alpha}\right)\{\dot{\mathbf{q}}\}^i + \left(1 - \frac{\delta}{2\alpha}\right)\Delta t\{\ddot{\mathbf{q}}\}^i + \frac{\delta}{\alpha \Delta t}(\{\mathbf{q}\}^{i+1} - \{\mathbf{q}\}^i) \tag{51}$$

where Δt is the time interval between the ith and $i+1$th time step, and α, δ are the parameters to be chosen for numerical stability. When $\alpha = 0.25$, $\delta = 0.5$, the scheme is unconditionally stable, and those were the values used here.

Substituting $\{\ddot{\mathbf{q}}\}^{i+1}$, $\{\dot{\mathbf{q}}\}^{i+1}$ into (48) evaluated at the $i+1$th time step, we get a system of $n + m$ equations in $\{\mathbf{q}\}^{i+1}$ and $\{\lambda\}^{i+1}$:

$$\frac{1}{\alpha(\Delta t)^2}[M]^{i+1}\{\mathbf{q}\}^{i+1} + ([\Phi_q]^T)^{i+1}\{\lambda\}^{i+1} = \{\mathbf{f}\}^{i+1} + [M]^{i+1}\{\Omega\}^i \tag{52}$$

$$\frac{1}{\alpha(\Delta t)^2}[\Phi_q]^{i+1}\{\mathbf{q}\}^{i+1} = \{\mathbf{h}\}^{i+1} + [\Phi_q]^{i+1}\{\Omega\}^i \tag{53}$$

where

$$\{\Omega\}^i = \frac{1}{\alpha(\Delta t)^2}\{\mathbf{q}\}^i + \frac{1}{\alpha \Delta t}\{\dot{\mathbf{q}}\}^i + \left(\frac{1}{2\alpha} - 1\right)\{\ddot{\mathbf{q}}\}^i$$

Feeding back the constraint violations at the ith step, (53) gives:

$$\frac{1}{\alpha(\Delta t)^2}[\Phi_q]^{i+1}\{\mathbf{q}\}^{i+1} = \{\mathbf{h}\}^{i+1} + [\Phi_q]^{i+1}\{\Omega\}^i - 2\gamma[\dot{\Phi}]^i + \beta^2[\Phi]^i \tag{54}$$

$\{\mathbf{q}\}^{i+1}$ and $\{\lambda\}^{i+1}$ can then be solved from (52) and (54). Once $\{\mathbf{q}\}^{i+1}$ is solved, $\{\dot{\mathbf{q}}\}^{i+1}$ and $\{\ddot{\mathbf{q}}\}^{i+1}$ can be determined from (50) and (51).

Before (52) and (54) can be solved, one needs to know the initial conditions for $\{\ddot{\mathbf{q}}\}$ and $\{\lambda\}$. For given initial conditions $\{\mathbf{q}\}_0$ and $\{\dot{\mathbf{q}}\}_0$, the initial value of $\{\lambda\}$ can be determined by substituting the $\{\ddot{\mathbf{q}}\}$ obtained from (44) into (47):

$$[\Phi_q]_0[M]_0^{-1}[\Phi_q]_0^T\{\lambda\}_0 = [\Phi_q]_0[M]_0^{-1}\{\mathbf{f}\}_0 - \{\mathbf{h}\}_0 \tag{55}$$

where the subscript 0 denotes the values evaluated at $t = 0$.

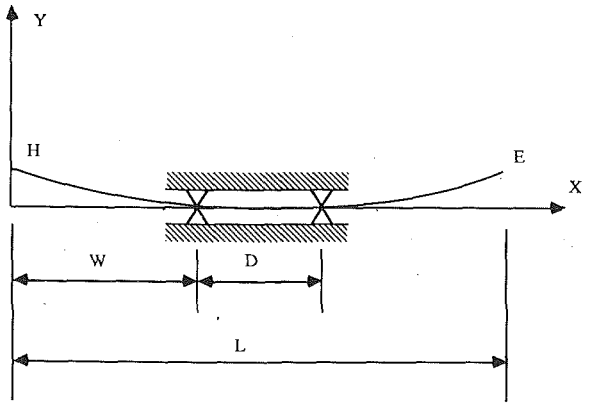

Fig. 6 Beam moving over bilateral supports

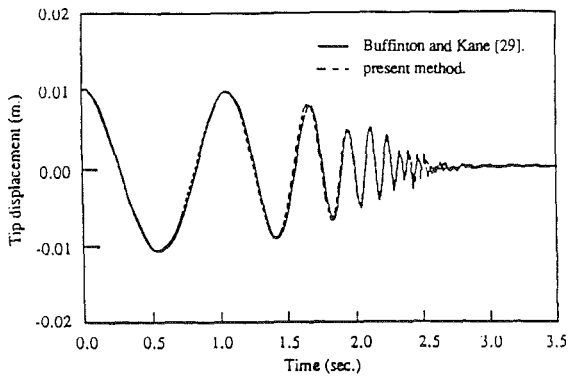

Fig. 7 Tip displacement in "slow push" case with C_1 = 0.725 m, C_2 = 0.7 m and T = 3.5 sec.

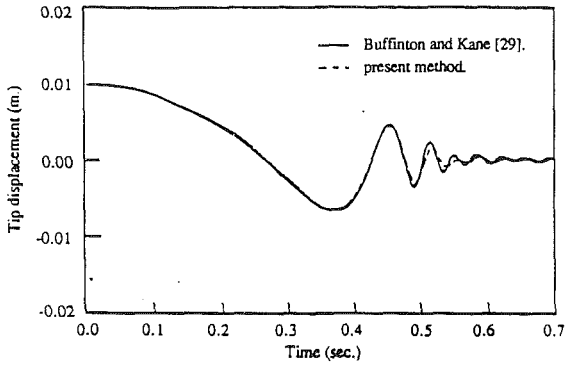

Fig. 8 Tip displacement in "fast push" case with C_1 = 0.725 m; C_2 = 0.7 m and T = 0.7 sec.

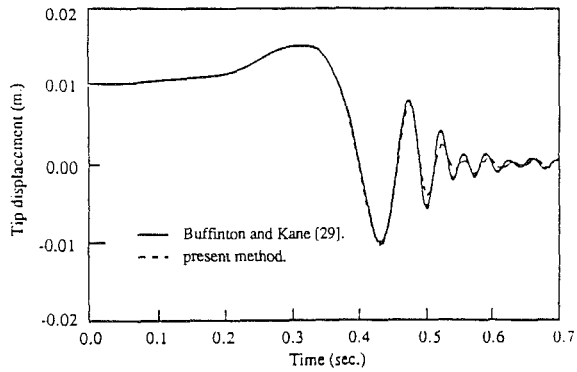

Fig. 9 Tip displacement in "fast pull" case with C_1 = 0.025 m, C_2 = −0.7 m and T = 0.7 sec.

The initial values of $\{\ddot{\mathbf{q}}\}_0$ can be determined from (44) after solving for $\{\lambda\}_0$:

$$\{\ddot{\mathbf{q}}\}_0 = [M]_0^{-1}(\{\mathbf{f}\}_0 - [\Phi_q]_0^T\{\lambda\}_0) \tag{56}$$

5 Example

An example adopted from Buffinton and Kane's work [29], is used to validate the modeling and numerical procedures discussed above. In this example, a uniform elastic beam of fixed length as shown in Fig. 6 is moving longitudinally over two bilateral supports and vibrating transversely. Initially, the beam is deformed by a uniform distributed load. At t = 0, the load is removed and the beam starts moving longitudinally with a prescribed speed. The parameters used in this example are: D = 0.25 m is the distance between the supports, ρ = 1.0 kg/m is the mass per unit length of the beam, L = 1.0 m is length of the beam, and EI = 1.0 N-m^2 is the flexural rigidity of the beam. The initial transverse displacement y of the beam is given in [29] (which is the static deflection due to a uniform load with a magnitude such that the deflection of the tip H is .01 m), and the initial velocity is $\dot{y}_0$ = 0.

Buffinton and Kane [29] treated several prescribed time histories. The one selected here for comparison is the one in which the beam starts from rest and is brought to rest in time T at a new longitudinal position. The longitudinal motion of the beam, in meters, is prescribed by the function [29]:

$$W = C_1 - \frac{C_2}{T}\left[t - \frac{T}{2\pi}\sin\left(\frac{2\pi t}{T}\right)\right] \tag{57}$$

where C_1 specifies the initial position of the beam, C_2 is the distance traveled by the beam, and T is the duration of the maneuver.

Four simple beam elements with the same length are used here for the finite element modeling. The first case studied is the so-called "slow push"; in which C_1 = 0.725 m, C_2 = 0.7 m and T = 3.5 sec. This corresponds to a maximum prescribed speed of 0.4 m/sec. The present result and Buffinton and Kane's result for the transverse displacement of point H are presented in Fig. 7, and show excellent agreement. Results for a "fast push" (peak speed 2 m/sec.), with C_1 = 0.725 m., C_2 = 0.7 m., T = 0.7 sec., are shown in Fig. 8. On the whole, very good agreement is seen, with slight disagreement in the region greater than 0.5 sec. (not regarded as important, since the amplitudes there are so small). Figure 9 presents the transverse tip displacement of point E (see Fig. 6) for a "fast pull", as opposed to push. In this case, the initial transverse displacement of the beam is given as the static deflection due to a uniform load with a magnitude such that the deflection of tip E is 0.01 m. The parameters for the longitudinal motion are C_1 = 0.025 m. C_2 = −0.7 m., T = 0.7 sec. (peak speed of 2 m/sec.). The response is quite different from the "push" cases, and very good overall agreement is still observed. It is interesting to note that if the axial shortening effects had been neglected, then the responses to "push" and "pull" cases would be identical. The conclusion to be drawn is that in high speed operation of flexible mechanisms, the retention of this effect can be important. The fact that very good agreement was found for all cases compared lends confidence to the current modeling approach, numerical procedure, and computer code.

6 Summary and Conclusions

In the proposed modeling procedure, a displacement based finite element method is employed to discretize the small displacement resulting from the flexibility of the links, and kinematic constraint equations are used to describe the compatibility conditions associated with both revolute and prismatic joints. Combining these two features, the procedure

gives us a model suitable for flexible links with prismatic joints. Another feature of this procedure is that the shortening effect of the link, accounting for the effect due to axial inertial forces, is included in the model. The importance of this effect has been seen from the example on the vibration of an axially moving beam over bilateral supports. The formulation permits the use of prescribed rigid body motions (partial coupling), or prescribed torques/forces (full coupling) as appropriate.

A numerical scheme combining the constraint stabilization method, and the Newmark direct integration method, is employed to solve the differential algebraic equations resulting from the equations of motion and the kinematic constraint equations. Excellent agreement is found with examples previously presented in the literature, lending confidence to the solution procedure.

In [30] experiments on a spherical coordinate robot, carried out to validate the model proposed here, and numerical simulations performed to study modeling issues related to flexible manipulators are reported.

7 References

1 Luh, J. Y. S., Walker, M. W., and Paul, R. P. C., "On Line Computational Scheme for Mechanical Manipulators," ASME *Journal of Dynamic Systems, Measurement, and Control*, Vol. 102, June 1980, pp. 69–76.

2 Hollerbach, J. M., "A Recursive Lagrangian Formulation of Manipulator Dynamics and A Comparative Study of Dynamics Formulation Complexity," *IEEE Transactions on Systems, Man and Cybernetics*, Vol. SMC-10, No. 11, Nov. 1980, pp. 730–736.

3 Likins, P. W., "Finite Element Appendage Equations for Hybrid Coordinate Dynamic Analysis," *International Journal of Solid and Structures*, Vol. 8, 1972, pp. 709–731.

4 Canavin, J. R., and Likins, P. W., "Floating Reference Frames for Flexible Spacecraft," *AIAA Journal of Spacecraft and Rocket*, Vol. 14, No. 12, December, 1977, pp. 724–732.

5 Book, W. J., "Analysis of Massless Elastic Chains with Servo Controlled Joints," ASME *Journal of Dynamic Systems, Measurement, and Control*, Vol. 101, Sept. 1979, pp. 187–192.

6 Nath, P. K., and Ghosh, A., "Kineto-Elastodynamic Analysis of Mechanisms by Finite Element Method," *Mechanism and Machine Theory*, Vol. 15, 1980, pp. 179–197.

7 Song, J. O., and Haug, E. J., "Dynamic Analysis of Planar Flexible Mechanisms," *Computer Methods in Applied Mechanics and Engineering*, Vol. 24, 1980, pp. 359–381.

8 Thompson, B. S., and Sung, C. K., "A Variational Formulation for the Nonlinear Finite Element Analysis of Flexible Linkages: Theory, Implementation, and Experimental Results, ASME JOURNAL OF MECHANISMS, TRANSMISSIONS, AND AUTOMATION IN DESIGN, Vol. 106, Dec. 1984, pp. 482–488.

9 Sunada, W., and Dubowsky, S., "The Application of Finite Element Method to the Dynamic Analysis of Flexible Spatial and Co-Planar Linkage Systems," ASME *Journal of Mechanical Design*, Vol. 103, July 1981, pp. 643–651.

10 Shabana, A., and Wehage, R. A., "Variable Degree-of-Freedom Component Mode Analysis of Inertia Variant Flexible Mechanical System," ASME JOURNAL OF MECHANISMS, TRANSMISSIONS, AND AUTOMATION IN DESIGN, Vol. 105, Sept. 1983, pp. 371–378.

11 Shabana, A., and Wehage, R. A., "Spatial Transient Analysis of Inertia-Variant Flexible Mechanical System," ASME JOURNAL OF MECHANISMS, TRANSMISSIONS, AND AUTOMATION IN DESIGN, Vol. 106, June 1984, pp. 172–178.

12 Turcic, D. A., and Midha, A., "A Generalized Equations of Motions for the Dynamic Analysis of Elastic Mechanism Systems," ASME *Journal of Dynamic Systems, Measurement, and Control*, Vol. 106, Dec. 1984, pp. 24-3–248.

13 Sunada, W., and Dubowsky, S., "On the Dynamic Analysis and Behavior of Industrial Robotic Manipulators with Elastic Members," ASME JOURNAL OF MECHANISMS, TRANSMISSIONS, AND AUTOMATION IN DESIGN, Vol. 105, March 1983, pp. 42–51.

14 Geradin, M., Robert, G., and Bernardin, C., "Dynamic Modelling of Manipulator with Flexible Members," *Advanced Software in Robotics*, Elsevier Science Publishers B. V. (North-Holland), 1984.

15 Book, W. J., "Recursive Lagrangian Dynamics of Flexible Manipulator Arms," *The International Journal of Robotics Research*, Vol. 3, No. 3, Fall 1984, pp. 87–101.

16 Judd, R. P., and Falkenburg, D. R., "Dynamics of Nonrigid Articulated Robot Linkages," *IEEE Transactions on Automatic Control*, Vol. AC-30, No. 5, May 1985, pp. 499–502.

17 Chalhoub, N. G., and Ulsoy, A. G., "Dynamic Simulation of a Leadscrew Driven Flexible Robot Arm and Controller," ASME *Journal of Dynamic Systems, Measurement, and Control*, Vol. 108, No. 2, June 1986, pp. 119–126.

18 Wang, P. K. C., and Wei, J., "Vibrations in A Moving Flexible Robot Arm," *Journal of Sound and Vibration*, 116(1), 1987, pp. 149–160.

19 Dym, C. L., and Shames, I. H., *Solid Mechanics—A Variational Approach*, McGraw-Hill, 1973.

20 Meirovitch, L., *Computational Methods in Structural Dynamics*, Sijthoff and Noordhoff, 1980.

21 Pan, Y. C., *Dynamic Simulation of Flexible Robots with Prismatic Joints*, Ph.D. Thesis, University of Michigan, Jan. 1988.

22 Cook, R. D., *Concepts and Applications of Finite Element Analysis*, John Wiley & Sons, New York, 1981.

23 Yigit, A., Scott, R. A., and Ulsoy, A. G., "Flexural Motion of A Radially Rotating Beam Attached to A Rigid Body," *Journal of Sound and Vibration*, Vol. 121, No. 2, 1988, pp. 201–210.

24 Gear, C. W., "Simultaneous Numerical Solution of Differential-Algebraic Equations," *IEEE Trans. Circuit Theory*, CT-18, (1), 1971, pp. 89–95.

25 Gear, C. W., "Differential-Algebraic Equations, Computer Aided Analysis and Optimization of Mechanical System Dynamics," *NATO ASI Series*, Vol. F9, 1984, pp. 323–334.

26 Petzold, L., "Differential/Algebraic Equations are not ODE's," *SIAM J. Sci. Stat. Comp.*, 3, 1982, pp. 367–384.

27 Baumgarte, J., "Stabilization of Constraints and Integrals of Motion in Dynamical Systems," *Computer Methods in Applied Mechanics and Engineering*, 1972, pp. 1–16.

28 Nikravesh, P. E., "Some Methods for Dynamic Analysis of Constrained Mechanical Systems: A Survey," *NATO AIS Series*, Vol. F9, 1984, pp. 351–367.

29 Buffinton, K. W., and Kane, T. R., "Dynamics of A Beam Moving Over Supports," *International Journal of Solids Structures*, Vol. 21, No. 7, 1985, pp. 617–643.

30 Pan, Y. C., Ulsoy, A. G., and Scott, R. A., "Experimental Model Validation for a Flexible Robot with a Prismatic Joint," ASME JOURNAL OF MECHANICAL DESIGN, Vol. 112, No. 3, Sept. 1990, pp. 315–323.